1-1-2014

Charged-controlled separation of nitrogen from natural gas using boron nitride fullerene

Qiao Sun
University of Wollongong, qsun@uow.edu.au

Caixia Sun
East China University of Science and Technology

Aijun Du
University of Queensland, Queensland University of Technology

Zhen Li
University of Wollongong, zhenl@uow.edu.au

Charged-controlled separation of nitrogen from natural gas using boron nitride fullerene

Abstract

Natural gas (the main component is methane) has been widely used as a fuel and raw material in industry. Removal of nitrogen (N_2) from methane (CH_4) can reduce the cost of natural gas transport and improve its efficiency. However, their extremely similar size increases the difficulty of separating N_2 from CH_4. In this study, we have performed a comprehensive investigation of N_2 and CH_4 adsorption on different charge states of boron nitride (BN) nanocage fullerene, $B_{36}N_{36}$, by using a density functional theory approach. The calculational results indicate that $B_{36}N_{36}$ in the negatively charged state has high selectivity in separating N_2 from CH_4. Moreover, once the extra electron is removed from the BN nanocage, the N_2 will be released from the material. This study demonstrates that the $B_{36}N_{36}$ fullerene can be used as a highly selective and reusable material for the separation of N_2 from CH_4. The study also provides a clue to experimental design and application of BN nanomaterials for natural gas purification.

Keywords

controlled, separation, nitrogen, natural, charged, gas, fullerene, boron, nitride

Disciplines

Engineering | Physical Sciences and Mathematics

Publication Details

Sun, Q., Sun, C., Du, A. & Li, Z. (2014). Charged-controlled separation of nitrogen from natural gas using boron nitride fullerene. The Journal of Physical Chemistry C: Energy Conversion and Storage, Optical and Electronic Devices, Interfaces, Nanomaterials, and Hard Matter, 118 (51), 30006-30012.

Charged-controlled Separation of Nitrogen from Natural Gas Using Boron Nitride Fullerene

Qiao Sun,[*†,‡] Caixia Sun,[‖] Aijun Du[§] and Zhen Li[*†,‡]

[†]School for Radiological and Interdisciplinary Sciences, Soochow University, Suzhou 215123, China

[‡]Institute of Superconducting & Electronic Materials, The University of Wollongong, NSW 2500, Australia.

[‖]Key Laboratory for Ultrafine Materials of the Ministry of Education, Shanghai Key Laboratory of Advanced Polymeric Materials, School of Materials Science and Engineering, East China University of Science and Technology, Shanghai 200237, China.

[§]School of Chemistry, Physics and Mechanical Engineering, Queensland University of Technology, Brisbane, QLD 4001, Australia.

Abstract: Natural gas (the main component is methane) has been widely used as a fuel and raw material in industry. Removal of nitrogen (N_2) from methane (CH_4) can reduce the cost of natural gas transport and improve its efficiency. However, their extremely similar size increases the difficulty of separation N_2 from CH_4. In this study, we have performed a comprehensive investigation of N_2 and CH_4 adsorption on different charge states of boron nitride (BN) nanocage fullerene, $B_{36}N_{36}$, by using a density functional theory approach. The calculational results indicate that $B_{36}N_{36}$ in the negatively charged state has high selectivity in separating N_2 from CH_4. Moreover, once the extra electron is removed from the BN nanocage, the N_2 will be released from the material. This study demonstrates that the $B_{36}N_{36}$ fullerene can be used as a highly selective and reusable material for the separation of N_2 from CH_4. The study also provides a clue to experimental design and application of BN nanomaterials for natural gas purification.

1. Introduction

Natural gas is a high efficiency fuel and an important raw material in the manufacturing of fertilizer, antifreeze, plastics, pharmaceuticals, fabrics, etc. Moreover, natural gas is the cleanest fossil fuel, because it has less CO_2 emission than either coal or oil and it produces fewer pollutants gases than other hydrocarbon fuels,[1] so that the demand for natural gas is continuously increasing. Natural gas needs to be transported, either by pipelines or by tankers, from the gas reservoirs to the final market, under the condition that the natural gas must contain at least 75% methane.[2] Nitrogen is a common component in natural gas and lowers its value. For natural gas transport by pipeline, typically, the nitrogen content needs to be less than 4%. In order to remove nitrogen from natural gas, several technologies have been used, including membrane separation, cryogenic removal, and solid adsorbents. Membrane separation isn't effective because of the very similar sizes of their molecules, as the kinetic diameters of N_2 and CH_4 are 3.64 Å and 3.80 Å, respectively.[3] Removal of nitrogen through cryogenic technology is an expensive process, which limits large-scale natural gas purification.[4] Recently, solid materials have been proposed as adsorbents for natural gas purification.[5] The interactions between most solid adsorbents and N_2 are relatively weak, however, so they cannot effectively separate nitrogen from methane.[6] Moreover, using a material with high nitrogen selectivity means that nitrogen release is difficult due to the strong interaction between nitrogen and the material, and the adsorbent cannot be reused. Therefore, it is very important to design new materials with high selectivity towards nitrogen removal from natural gas and easy regeneration in order to allow the reuse of these materials.

Fullerene-based materials have attracted considerable attention because of their excellent properties, such as physical and chemical stability. Stoichiometric boron nitrides $(BN)_n$, the isoelectronic analogues to the carbon fullerenes, have been the subject of extensive and intensive investigations.[7-10] The four-fold ring-type $B_{36}N_{36}$ is considered as a local model for the octahedral-like "family" of BN fullerenes that has been experimentally[11] observed and theoretically[8] investigated. Several theoretical studies indicate that $B_{36}N_{36}$ is energetically[12,13] and vibrationally[13] stable, The most stable structure of $B_{36}N_{36}$ has a T_d symmetry with 6 four-membered (F_4) and 32 six-membered (F_6) rings.[14] BN fullerenes have properties that could make their use viable in electronic devices or as semiconductors with high chemical and thermal stability. For example, $B_{36}N_{36}$ has been studied extensively as a material for hydrogen storage,[9,15] drug delivery,[16] and natural gas storage[17]. One potential application of $B_{36}N_{36}$ is its use as an adsorbent for the selective separation of nitrogen from methane for natural gas purification. The interaction between neutral $B_{36}N_{36}$ and N_2 is very weak, however, when one electron was introduced onto the system, strong interaction between $B_{36}N_{36}$ and N_2 could occur. Regardless of whether the $B_{36}N_{36}$ nanocage is in a charged or neutral state, the CH_4 always takes part in only a weak interaction with it. This study demonstrates that $B_{36}N_{36}$ in the negative charge state has high selectivity towards the separation of nitrogen from methane. We also investigated the reaction mechanism for the removal of charge from the $B_{36}N_{36}$. Once

the negative charge is removed from the BN adsorbent, the N_2 will be released from the BN nanocage. This investigation demonstrates that the BN nanocage can effectively separate nitrogen from a mixture with methane. Furthermore, by switching the charge state off, nitrogen will be released from the material, and the BN nanomaterial can be reused for further separation. Here, we need to point out that the charge state of BN nanomaterial can be modified through electrochemical methods, electron beams, electrospraying, or gate voltage control.[18-20]

2. Computational Methods

The investigations have been carried out using first-principles density functional theory plus dispersion correction, as implemented in the DMol3 module in Materials Studio,[21,22] to calculate the structure and energy of the $B_{36}N_{36}$–N_2 and $B_{36}N_{36}$–CH_4 systems. We used the generalized gradient approximation[23] treated by the Perdew-Burke-Ernzerhof exchange-correlation potential in density functional theory, with long range dispersion correction via Grimme's scheme[24] (PBE-D) for all the calculations. An all electron double numerical atomic orbital augmented by *d*-polarization functions (DNP) has been chosen as basis set. This calculational level has been used to successfully study adsorptions, desorption and the reaction mechanisms of some gases on boron-containing nanomaterials.[5,25-28]

The adsorption energies (E_{ads}) of N_2 and CH_4 on $B_{36}N_{36}$ are calculated from Eq. (1):

$$E_{ads} = (E_{B36N36} + E_{gas}) - E_{B36N36\text{-}gas} \quad (1)$$

where $E_{B36N36\text{-}gas}$ is the total energy of the $B_{36}N_{36}$ with the adsorbed gas, E_{B36N36} is the energy of isolated $B_{36}N_{36}$, and E_{gas} is the energy of an isolated gas molecule, such as N_2 and CH_4. All the adsoptions energies are calculated based on their charge states of the adsorbent. The Mulliken method is used to determine the electron distribution and charge transfer of the adsorptions.[29]

In order to study the nature of the interactions between N_2, CH_4 and $B_{36}N_{36}$ with different charge states, the atoms in molecules (AIM) theory, which has been used to successfully determine the existence and strength of bonds in different gases and nanomaterial systems, has been employed in this system.[30-32] The topological analysis of $B_{36}N_{36}$-gas has been performed by using the AIMALL code.[32] Please refer to our previous publication[27] for detailed information on the computational methods used in the system that is the object of the current study.

3. Results and Discussion

In order to evaluate the ability of the $B_{36}N_{36}$ nanocage to separate nitrogen from methane, we firstly performed PBE-D calculations for the adsorption of the gases, N_2 and CH_4, on a neutral $B_{36}N_{36}$ nanocage. We have performed the calculations with all possible configurations of the gases adsorbed on the $B_{36}N_{36}$, the computational results show that the interactions between N_2/CH_4 molecules and the neutral $B_{36}N_{36}$ are very weak. Then, we analyzed the frontier orbitals of $B_{36}N_{36}$ and difference in the electron densities between the neutral and 1 e^- charge states of $B_{36}N_{36}$. The analysis of the frontier orbitals suggests that N_2 may form a strong interaction with 1 e^- charged $B_{36}N_{36}$. The calculations for N_2 capture on negatively charged $B_{36}N_{36}$ then followed. Finally, we also have studied the release of N_2 on $B_{36}N_{36}$ when the charge state is turned off, and compared the adsorption of N_2 and CH_4 on $B_{36}N_{36}$ in different charge states in order to address the high selectivity and reusability of the BN adsorbent for nitrogen removal in natural gas purification.

3.1 N_2 and CH_4 adsorption on uncharged $B_{36}N_{36}$ nanocage

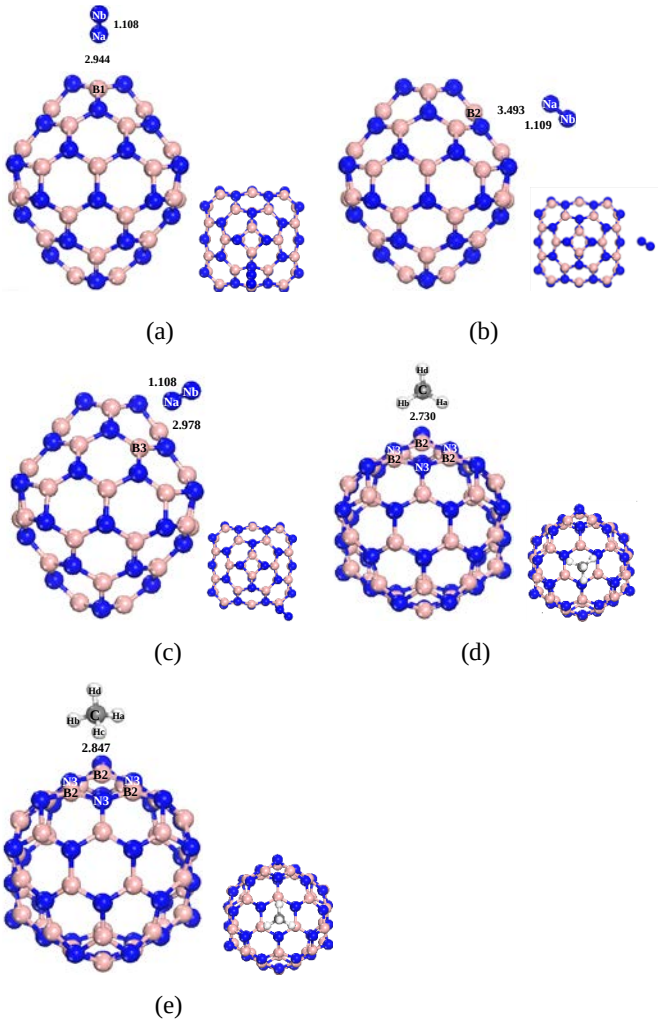

Figure 1. Top and side views of three physisorbed configurations: type 1 (a), type 2 (b), and type 3 (c) of N_2 on $B_{36}N_{36}$ in its neutral state. Top and side views of two most stable configurations of CH_4 adsorption on $B_{36}N_{36}$ in its neutral state (d, e). Atom color code: blue, nitrogen; pink, boron; gray, carbon; white, hydrogen.

We have carried out PBE-D calculations of N_2 and CH_4 adsorption on uncharged $B_{36}N_{36}$ nanocage with all the possible configurations, and the calculated complexes are shown in Figure 1. For N_2 adsorption on uncharged $B_{36}N_{36}$ nanocage, the three most stable structures formed between N_2 and the uncharged $B_{36}N_{36}$, with one boron atom belonging to the F_4 ring and two boron atoms belonging to F_6 rings, are denoted as type 1 (Figure 1(a)), type 2 (Figure 1(b)), and type 3 (Figure 1(c)), respectively. The important geometry structural parameters and the adsorption energies are summarized in Table 1

accordingly. In the three configurations formed by N_2 and uncharged $B_{36}N_{36}$ (Figure 1), the N_2 molecules are far from the $B_{36}N_{36}$, with contact distances from 2.944 Å to 3.493 Å. The

Table 1. Adsorption energy in kcal/mol, bond distance (*r*) in Å, and bond angle (*α*) in degrees of N_2 and CH_4 adsorption on $B_{36}N_{36}$ in different charge states.

Gases			0e	$1e^-$
N_2	Type 1	Adsorption energy	-3.32	-15.73
		r(B…Na)	2.944	1.622
		r(Na–Nb)	1.108	1.168
		α(Nb–Na–B)	177.6	131.9
N_2	Type 2	Adsorption energy	-3.25	-9.00
		r(B…Na)	3.493	1.718
		r(Na–Nb)	1.109	1.167
		α(Nb–Na–B)	127.9	123.3
N_2	Type 3	Adsorption energy	-2.32	-11.30
		r(B…Na)	2.978	1.662
		r(Na–Nb)	1.108	1.167
		α(Nb–Na–B)	157.2	127.6
CH_4	Type 1	Adsorption energy	-4.51	-4.33
		r(N…C)	3.475	3.478
		r(N…H)	2.730	2.723
CH_4	Type 2	Adsorption energy	-4.41	-4.23
		r(B…C)	3.385	3.391
		r(B…H)	2.847	2.841

Table 2. Mulliken charge distribution (electron) of configurations of N_2 and CH_4 adsorption on $B_{36}N_{36}$ and the net charge (NC) of N_2 and CH_4 in the adsorbed configurations.

Gases			0e	$1e^-$
N_2	Type 1	Na	-0.026	-0.177
		Nb	0.040	-0.105
		NC	0.014	-0.282
N_2	Type 2	Na	-0.006	-0.122
		Nb	0.011	-0.188
		NC	0.005	-0.310
N_2	Type 3	Na	-0.017	-0.112
		Nb	0.026	-0.187
		NC	0.009	-0.299
CH_4	Type 1	C	-0.397	-0.392
		Ha	0.103	0.105
		Hb	0.100	0.100
		Hc	0.102	0.105
		Hd	0.099	0.077
		NC	0.007	-0.005
CH_4	Type 2	C	-0.396	-0.391
		Ha	0.104	0.106
		Hb	0.102	0.101
		Hc	0.105	0.106
		Hd	0.099	0.076
		NC	0.014	-0.002

N-N bond distances in the three complexes vary between 1.108 Å and 1.109 Å, which are close to that in the gas phase (where the N-N bond length of the free N_2 molecule is calculated to be 1.109 Å). From the configurations in Figure 1 and the data in Table 1 we can see that the three complexes formed between N_2 and $B_{36}N_{36}$ are physisorbed configurations. Figure S1 in the Supporting Information lists the molecular graphs of those geometries. From Figure S1(a-c) we can see that there are bond critical points (BCP) at the N-B interactions of the three configurations of N_2 adsorption on the neutral $B_{36}N_{36}$. The relevant topological parameters at the BCP are listed in Table S1 in the Supporting Information. The small electron densities at the BCPs of the N-B contacts of the three structures (Table S1) clearly indicate that the interactions between N_2 and $B_{36}N_{36}$ are weak. The Mulliken charge distributions of the complexes of N_2 adsorption on the $B_{36}N_{36}$ nanocage and the charge transfers between N_2 and $B_{36}N_{36}$ are listed in Table 2. We can see that the charge transfers for the three physisorbed configurations from N_2 to $B_{36}N_{36}$ are negligible, with the values ranging from 0.005 e to 0.014 e. The adsorption energies of the three configurations for N_2 molecule adsorption on neutral $B_{36}N_{36}$ are calculated to be 3.32, 3.25, and 2.32 kcal/mol, which are in good agreement with the weak interactions between N_2 and the uncharged $B_{36}N_{36}$ nanocage. To sum up, the calculations data demonstrates that there are weak interactions between N_2 and neutral $B_{36}N_{36}$.

We also investigated the adsorption of CH_4 on neutral $B_{36}N_{36}$. Starting with all possible configurations, the two most stable structures between CH_4 and neutral $B_{36}N_{36}$ are presented in Figure 1(d) and Figure 1(e). For these two structures, their most important geometrical parameters, adsorption energies, and electron transfer from $B_{36}N_{36}$ to CH_4 are summarized in Table 1 and 2. From the Figure 1 and the Tables we can see that CH_4 is quite far from the $B_{36}N_{36}$ for the two configurations of CH_4 adsorbed on neutral $B_{36}N_{36}$ nanocage, and the N/B…H distances are 2.730 Å and 2.847 Å for the two configurations, respectively. There are small values of electron transfer from methane to $B_{36}N_{36}$ of 0.007 e and 0.014 e for the two complexes. The adsorption energies for the two complexes are 4.51 kcal/mol and 4.41 kcal/mol. The above analysis demonstrates that the adsorptions of CH_4 on neutral $B_{36}N_{36}$ are physical interactions, and the interactions are weak, which is supported by the topological analysis in the AIM calculations. Figure S1 in the Supporting Information shows there are BCP of the H-B contact between CH_4 and neutral $B_{36}N_{36}$. Similarly to the electron densities at the BCPs of $B_{36}N_{36}$–N_2 system, the values of H-B between CH_4 and the $B_{36}N_{36}$ nanocage are small (Table S1). This supports the position that there are only weak interactions between CH_4 and neutral $B_{36}N_{36}$. In all, the calculational results clearly demonstrate that the interactions between N_2/CH_4 and neutral $B_{36}N_{36}$ are very weak, so that neutral $B_{36}N_{36}$ cannot separate N_2 from a mixture with CH_4.

3.2 Frontier orbitals of $B_{36}N_{36}$ and charge distribution of $B_{36}N_{36}$ with different charge states

In order to understand the interactions between the neutral $B_{36}N_{36}$ nanocage and the gases, the frontier orbitals, the highest occupied molecular orbital (HOMO, Figure 2(a)) and the lowest unoccupied molecular orbital (LUMO, Figure 2(b)), of the $B_{36}N_{36}$ are displayed in Figure 2. The Figure 2(b) clearly shows that the LUMO of $B_{36}N_{36}$ is distributed on its boron atoms, which suggests that when an extra electron is applied to the $B_{36}N_{36}$ nanocage, the electron will migrate to the boron atoms of $B_{36}N_{36}$. The above prediction is confirmed by comparing the difference in the electron density distribution for the different

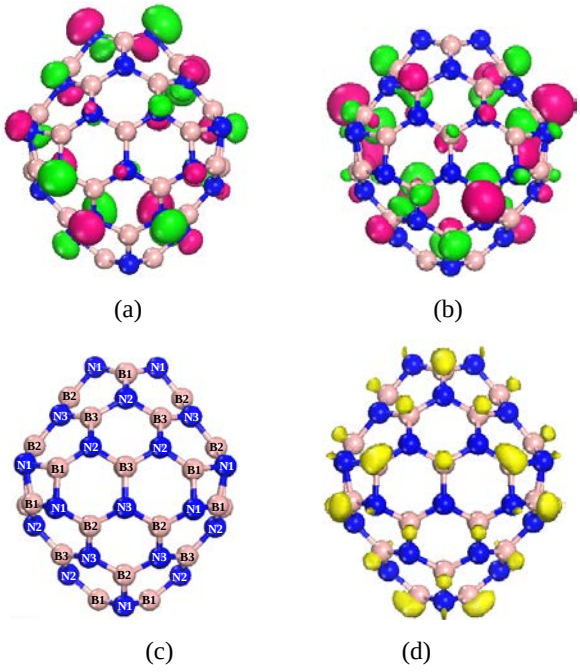

Figure 2. The HOMO (a) and LUMO (b) of $B_{36}N_{36}$. These orbitals are drawn with an isosurface value of 0.03e/Å^3. The colors of the orbitals show the wavefunction (green - positive, red - negative). (c) Atom types of $B_{36}N_{36}$ nanocage. The differences in electron density distributions (d) between 0 e^- and 1 e^- charge carrying states of $B_{36}N_{36}$. The density is drawn with an isosurface value of 0.008e/Å^3. Atom color code: blue, nitrogen; pink, boron.

charge states of $B_{36}N_{36}$. Figure 1(c) and Table S1 in the Supporting Information show the atom types of the $B_{36}N_{36}$ nanocage and the Mulliken charge distributions of the different atom types, respectively. From Figure 1(c), we can see that there are three types of boron and nitrogen atoms in the $B_{36}N_{36}$ nanocage: the type 1 atoms are denoted as B1 and N1 which are atoms belonging to the four- membered (F_4) rings; type 2 atoms are denoted as B2 and N_2, which are atoms belonging to six-membered (F_6) rings, which are directly connected with the atoms of the F_4 rings; type 3 atoms are denoted as B3 and N3, and they are atoms belonging to six-membered (F_6) rings and not connected with the atoms of F_4 rings. There are six types of bonds in the $B_{36}N_{36}$ fullerene. The distances of the six types of bonds are listed in Table S1 in supporting information. We can see that the six types of bonds in its negative charge state increase with the values among 0.001～0.004 Å compared with those in its neutral state, which mean that the cluster expands a little bit when it is negatively charged. The Mulliken charges of B1, B2, and B3 of neutral $B_{36}N_{36}$ are 0.297 e, 0.445 e and 0.481 e, and the charge distribution of the three types of atoms in 1e^- state $B_{36}N_{36}$ are 0.268 e, 0.424 e and 0.459 e, respectively. The boron atoms become negatively charged with the values of -0.029 e, -0.021 e, and -0.022 e, for the atom types B1, B2, and B3, respectively. The changes for the nitrogen atoms in the $B_{36}N_{36}$ are much smaller, however, than those for the boron atoms. For example, the Mulliken charges of N1, N2, and N3 in neutral and 1 e^- $B_{36}N_{36}$ are -0.362e, -0.420e, and -0.442e for neutral $B_{36}N_{36}$; and -0.376e, -0.420e, and -0.440e for negatively charged $B_{36}N_{36}$, respectively; the changes for the three types of atom between the two charge states are approximately 0–0.014 e. The difference in electron density distribution between the 0 e and 1 e^- $B_{36}N_{36}$ is shown in Figure 2(d). We can see from Figure 2(d) that when an extra electron is applied to the $B_{36}N_{36}$ nanocage, the electron is distributes to the boron atoms of $B_{36}N_{36}$, and then the negatively charged boron atom of $B_{36}N_{36}$ becomes more likely to donate an electron to N_2 than in its neutral state analogue, and N_2 is more likely to adsorb strongly on the negative charge state of $B_{36}N_{36}$. When the extra electron is moved from the $B_{36}N_{36}$ nanocage, the electron density of boron atoms will vanish accordingly, and then the strong adsorption of N_2 on $B_{36}N_{36}$ will not exit. The analysis indicates the changes of the charge states of the $B_{36}N_{36}$ nanocage might control its ability to capture/release N_2.

It is known that Mulliken charges have some shortcomings, such as they are very sensitive to the basis set. We have performed the Hirshfeld charge analysis because the charge states of $B_{36}N_{36}$ are vital to the performances of separation nitrogen from methane mixture. The Hirshfeld charges of $B_{36}N_{36}$ with neutral and 1e^- states at the PBE-D are listed in Table S1 in supporting information. From Table S1 we can see that Hirshfeld charges of the three types of boron atoms in 1e^- state are become negatively charged compared with them in its neutral state with the values of -0.023 e, -0.016 e, and -0.016 e, for the atom types B1, B2, and B3, respectively. The changes for the nitrogen atoms in the $B_{36}N_{36}$ with different charge states are much smaller than those for the boron atoms. The results of Hirshfeld charges are consistent with those of Mulliken charges.

3.3 N_2 and CH_4 adsorption on $B_{36}N_{36}$ with 1 e^- charge state

In this part, the investigation of N_2 and CH_4 adsorption on $B_{36}N_{36}$ in the 1 e^- charge state has been carried out. From the calculation results, we can see that there are three most stable configurations of N_2 adsorption on 1 e^- charge state $B_{36}N_{36}$, in the three boron positions, where the N_2 molecules interact with the three boron atoms of types B1, B2, and B3 of $B_{36}N_{36}$. The three configurations are shown in Figure 3(a-c), respectively. Their important geometrical parameters, adsorption energies, and charge transfer from N_2 to $B_{36}N_{36}$ are summarized in Tables 1 and 2. We can see from Figure 3 that N_2 molecules form strong interactions with 1 e^- charged $B_{36}N_{36}$, and there are chemisorbed configurations formed between them. In the three chemisorbed configurations of N_2 adsorption on the negative charge $B_{36}N_{36}$, the N-N bonds are slightly elongated from 1.109 Å (gas phase) to 1.168 Å, 1.167 Å, and 1.167 Å for the complexes with types 1, 2, and 3, respectively, and the triple-bonds of N_2 molecules in the three configurations are broken. The distances between B atoms and N atoms of the three configurations are 1.622 Å, 1.718 Å, and 1.662 Å for types 1, 2, and 3, respectively, which are shorter than those for N_2 adsorption on the neutral uncharged $B_{36}N_{36}$ (since the distances between N_2 and neutral $B_{36}N_{36}$ for types 1, 2, and 3 are 2.944 Å, 3.493 Å, and 2.978 Å, respectively). This indicates that the stronger interactions between N_2 and 1 e^- $B_{36}N_{36}$ are formed, which is also consistent with the relatively larger electron densities at the BCPs for the N-B bond in the three configurations (Figure S1 and Table S2 in the Supporting Infor-

mation). For the chemisorptions, the net charge via Mulliken charges analysis of N_2 part increases with the value of 0.282 e^-, 0.310 e^-, and 0.299 e^- for the three configurations of type 1, type 2, and type 3, respectively. The Hirshfeld charges of the configurations of N_2 and CH_4 adsorption on $B_{36}N_{36}$ with neutral and 1e^- states and the net charge (NC) of N_2 and CH_4 in the adsorbed configurations at the PBE-D are listed in Table S3 in supporting information. The NC via Hirshfeld charges distributions of these configurations are consistent with those of Mulliken charges analysis. The absorption energies of the three configurations of types 1, 2, and 3 are 15.73, 9.00, and 11.30 kcal/mol (or 65.75, 37.08, and 47.23 kJ/mol), respectively. The high adsorption energies indicate that there are strong interactions between N_2 and $B_{36}N_{36}$ in the 1 e^- charge state. Generally speaking, the adsorption energies of a good-performance adsorbent should be in a range of 40 – 80 kJ/mol,[33] which support the negatively charged $B_{36}N_{36}$ could be a good material for N_2 separation.

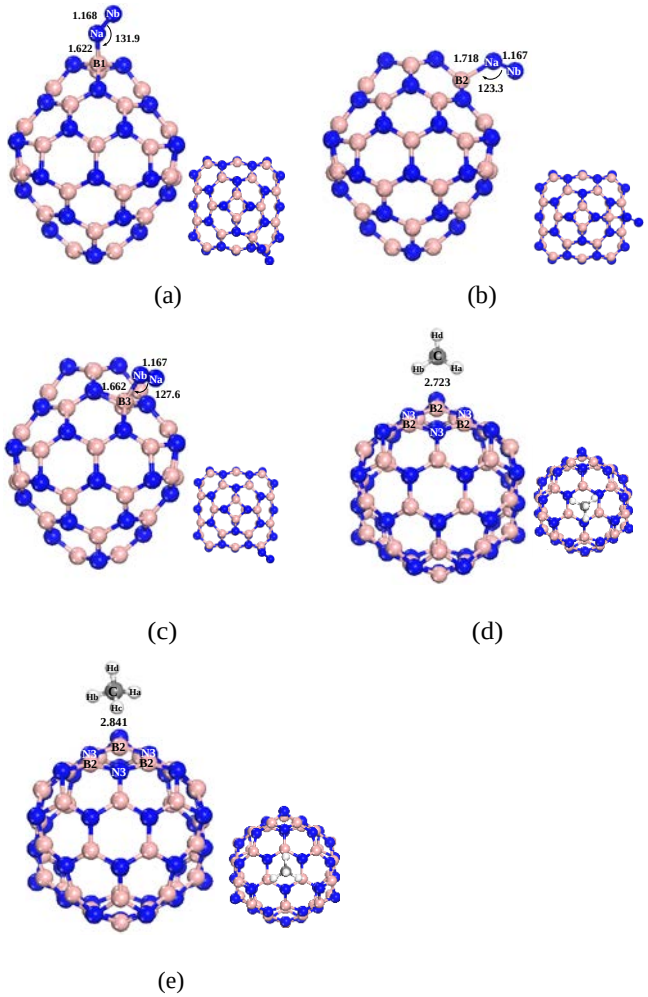

Figure 3. Top and side views of three chemisorbed configurations of type 1 (a), type 2 (b), and type 3 (c) of N_2 on $B_{36}N_{36}$ in the 1 e^- charge carrying state; (d) and (e) are top and side views of the two most stable configurations of CH_4 adsorption on $B_{36}N_{36}$ in the 1 e^- charge state.

In order to demonstrate the high-selectivity of the negatively charged $B_{36}N_{36}$ nanocage towards N_2 removal in neutral gas purification, the interactions between CH_4 and the 1 e^- charged state of $B_{36}N_{36}$ are calculated and compared with the properties of the configurations formed between neutral $B_{36}N_{36}$ and CH_4. Figure 3(d) and (e) are the two most stable configurations for CH_4 adsorptions on $B_{36}N_{36}$ in the 1 e^- charge state. The important geometrical parameters for these configurations, adsorption energies, and electron transfer for CH_4 adsorption on 1 e^- $B_{36}N_{36}$ are listed in Tables 1 and 2. From Figure 3 we can see that the configurations of CH_4 adsorption on negatively charged $B_{36}N_{36}$ are very similar to those for its neutral state. They are all physisorbed configurations with C…B distances in the range of 3.3 – 3.5 Å, and the weak interactions between CH_4 and $B_{36}N_{36}$ are supported by the small values of net charge of CH_4 part (in the range of 0.002e – 0.014e) and adsorption energies listed in Table 2, as well as the topological analysis from AIM calculations in the Supporting Information. This means that CH_4 can only form weak interactions with the $B_{36}N_{36}$ nanocage, no matter what the charge state of the adsorbent. In order to address the capability of $B_{36}N_{36}$ for N_2/CH_4 separation, the adsorption energies for CH_4 and N_2 adsorption on $B_{36}N_{36}$ in the different charge states will be compared. In detail, for neutral $B_{36}N_{36}$, the interactions with CH_4 and N_2 molecules on it are all physical. The adsorption energies of the five configurations of CH_4 and N_2 on neutral $B_{36}N_{36}$ are in the range of 4.2 – 4.5 kcal/mol. When the $B_{36}N_{36}$ nanocage is introduced with one electron, the interactions of CH_4 on $B_{36}N_{36}$ remain weak, and the changes in the adsorption energies are very small in comparison to those on its neutral state. The adsorption energies are ~4.3 kcal/mol for CH_4 on $B_{36}N_{36}$ nanocage in the 1 e^- charge state. In contrast, the interactions of N_2 on 1 e^- charged $B_{36}N_{36}$ are much stronger (since the complexes formed between them are chemisorbed configurations) than those of CH_4 adsorption on the charged $B_{36}N_{36}$ (where the complexes formed between them are physisorbed configurations). The adsorption energy of the most stable configuration (type 1 in Figure 3(a)) of N_2 adsorbed on the charged $B_{36}N_{36}$ is 15.73 kcal/mol. The big differences between these configurations and adsorption energies indicate that the negatively charged $B_{36}N_{36}$ has high selectivity towards removal of N_2 from CH_4, so $B_{36}N_{36}$ can serve as a good candidate for natural gas purification. Previously we have studied N_2 capture on solid boron, and we found that the adsorption energies of N_2 on the surfaces of the solid boron, such as α-B_{12} and γ-B_{28}, are among 25-27 kcal/mol,[5] which are larger than that of N_2 on $B_{36}N_{36}$ with 1 e^- charge state of this study. The comparison indicates that N_2 release from $B_{36}N_{36}$ is more feasible than those from solid α-B_{12} and γ-B_{28} because the regenerations are difficult with the large adsorption energies.

In order to know the influence of Grimme dispersion correction, we have also performed calculations of $B_{36}N_{36}$–CH_4 and $B_{36}N_{36}$–N_2 systems with neutral and 1e^- states at the PBE level without Grimme dispersion correction. The calculational results, such as adsorption energy and bond distance of N_2 and CH_4 adsorption on $B_{36}N_{36}$ with the two charge states at the PBE level are listed in Table S4 in

supporting information. The adsorption energies of the two gases on the adsorbent with neutral and 1e$^-$ states are weaker and bond distances between the gases and the adsorbent with the two states are longer at the PBE level than those of at the PBE-D level. Through the comparison of the differences of geometry and energy between the calculational methods with and without Grimme dispersion correction, we found that PBE-D is a reasonable calculational level for this study.

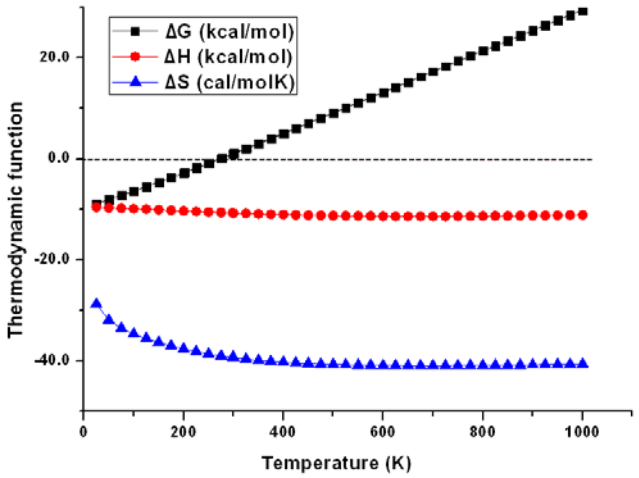

Figure 4. Variation of thermodynamic properties with temperatures (K) when an isolated N_2 molecule is chemisorbed by 1 e$^-$ charged $B_{36}N_{36}$ in a type 1 configuration. Squares, triangles, and circles correspond to the change in Gibbs free energy (kcal/mol), change in entropy (cal/mol K), and change in enthalpy (kcal/mol), respectively.

In order to study the thermodynamic properties of N_2 adsorption on $B_{36}N_{36}$ in the 1 e$^-$ charge state to form chemisorbed configurations under different temperature, the variations in the entropy (ΔS, cal/mol K), enthalpy (ΔH, kcal/mol), and Gibbs free energy (ΔG, kcal/mol) with temperature (K) have been studied. Here, we mainly discuss the thermodynamic properties of the reaction between N_2 and $B_{36}N_{36}$ in the 1 e$^-$ charged state to form the most stable configuration, in which N_2 is directly connected with an F4 boron atom of the charged $B_{36}N_{36}$, which is shown in Figure 4. From Figure 4 we can see that ΔS decreases with the temperature increasing from 25 to 300 K, and when the temperature is above 300 K, ΔS is almost constant. Over the whole temperatures range (i.e. from 25 to 1000 K), the value of ΔH is almost constant, which results in a linear increase in ΔG with increasing temperature. In addition, when the temperature is in the range of 25 – 300 K, ΔG is negative, which indicates that when the temperature is below 300 K, the adsorption of N_2 on 1 e$^-$ charged $B_{36}N_{36}$ to form a chemisorbed configuration is a spontaneous process. Figure S2(a) and (b) in the Supporting Information lists the thermodynamic properties of N_2 adsorption on the 1 e$^-$ charged $B_{36}N_{36}$ in the type 2 and type 3 configurations, in which N_2 is directly connected with the boron atoms of F_6 rings. Figure S2(a) and (b) shows that ΔG is positive when the temperature is above 200 K, which means that the reactions with the type 2 and type 3 configurations are not spontaneous at room temperature. To sum up, the analysis of the thermodynamic properties of the reaction to form the chemisorbed configuration (type 1) demonstrates that N_2 capture on 1 e$^-$ charged $B_{36}N_{36}$ is a spontaneous process when the temperature is below 300 K.

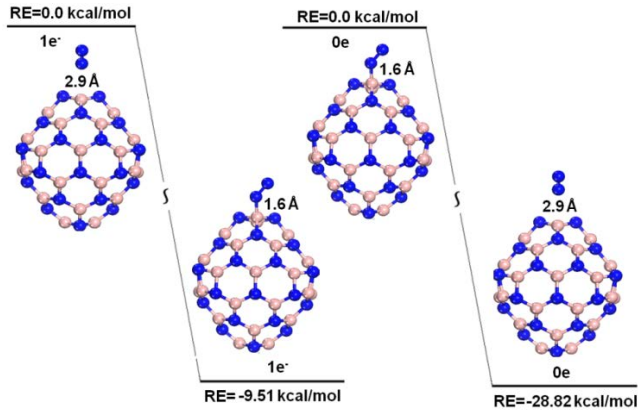

Figure 5. Energy change for reactions involving N_2 adsorption on $B_{36}N_{36}$ of type 1 (a) involves the change from physisorbed to chemisorbed configurations with the 1 e$^-$ charged $B_{36}N_{36}$, respectively; (b) is the change from physisorbed to chemisorbed configurations with the neutral $B_{36}N_{36}$.

We have also investigated the reaction mechanism of N_2 capture/release on/from $B_{36}N_{36}$ in different charge states, the energy changes for the reactions involving turning on/off the charge states of $B_{36}N_{36}$ of the three types of adsorptions are plotted in Figure 5 (type 1) and Figure S3 (type 2 and 3) in the Supporting Information. Figure 5(a) and (b) lists the energy changes in the type 1 configuration, in which N_2 molecules are connected with boron atoms of the F_4 ring of $B_{36}N_{36}$. Figure S3(a-d) shows the energy changes in the type 2 and type 3 configurations, in which the N_2 molecules are connected to the boron atoms of the F_6 ring of $B_{36}N_{36}$. The changes in energy with relaxation from physisorbed to chemisorbed states have been plotted in Figure 5 (a), Figure S3(a) and Figure S3 (c), when the electrons are added into the $B_{36}N_{36}$–N_2 systems. In Figure 5 (b), Figure S3(b) and Figure S3(d), starting with the minimum energy configurations of 1 e$^-$ charged $B_{36}N_{36}$ with chemisorbed N_2. When the electrons are removed, so that the systems are allowed to relax, the systems change from their chemisorbed to physisorbed N_2 adsorption configurations on $B_{36}N_{36}$. In detail, when the electrons are introduced onto the $B_{36}N_{36}$–N_2 systems, the interactions between N_2 and $B_{36}N_{36}$ dramatically increase compared with those with the neutral states, and the N_2 molecules are chemisorbed onto the $B_{36}N_{36}$. The calculation results (Figure 5 (a), Figure S3(a) and Figure S3 (c)) indicate that the processes are exothermic with the values of 9.51, 2.52 and 6.03 kcal/mol for the three types, respectively. On the other hand, after the negative charges are released from the systems, the adsorptions of N_2 on $B_{36}N_{36}$ spontaneously change from chemisorbed to physisorbed configurations (Figure 5(b), Figure S3(b) and

(d)), and the processes are still exothermic by 28.82, 36.75 and 33.54 kcal/mol for the three types of configurations, respectively. The above analysis demonstrates that the reactions are exothermic with these changes after the electrons are removed from the systems. We need to point out that the energy for promoting the adsorption/desorption processes are coming from the energy for charging/discharging of the $B_{36}N_{36}$. Once the charge states are turned on/off, both adsorption and release processes of N_2 on $B_{36}N_{36}$ are spontaneous. To sum up, our calculations demonstrate that the $B_{36}N_{36}$ could be a reusable nanomaterial for the removal of N_2 from CH_4 for neutral gas purification.

4. Conclusions

To the best of our knowledge, this is the first investigation of the reversible removal of N_2 from CH_4 by using boron nitride nanomaterial. The study demonstrates that N_2 adsorption on $B_{36}N_{36}$ can be dramatically enhanced by adding electrons to the adsorbent, which indicates that the negatively charged $B_{36}N_{36}$ is an excellent sorbent for the selective separation of N_2 from CH_4 for neutral gas purification. Moreover, the absorbed N_2 can be spontaneously released from the BN nanocage with no reaction barrier once the electron is released, so that the adsorbent can be reused. In summary, this study provides information on experimental research that BN nanomaterial and the approach of switching the charge state of the nanomaterial on/off can remove N_2 from CH_4 for natural gas purification, and the addition/removal of the negative charge to/from the sorbent can be easily realized experimentally.

Author Information

Corresponding Author

*E-mail: qiaosun@suda.edu.au; zhenli@suda.edu.cn

Acknowledgement

We acknowledge generous grants of high performance computer time from the National Computational Infrastructure (NCI) of Australia and Soochow University in China.

Supporting Information

Mulliken and Hirshfeld charges of $B_{36}N_{36}$ with different charge states, molecular graphs of the absorbed configurations and variation of thermodynamic properties with temperature of the systems at the PBE-D level as well as the important properties of $B_{36}N_{36}$–N_2 and $B_{36}N_{36}$–CH_4 systems calculated at the PBE level are listed in supporting information. This information is available free of charge via the Internet at http://pubs.acs.org.

References

(1) Natural Gas and the Environment. Naturalgas.org. Retrieved **2011-02-06**.

(2) Kidnay, A. J.; Parrish, W. R. Fundamentals of Natural Gas Processing, Taylor & Francis, *Boca Raton, USA*, ***2006***.

(3) Breck, D. W., Zeolite Molecular Sieves, *John Willey & Sons, New York, USA*, **1974**.

(4) Daimiger, U.; Lind, W. Adsorption Processes for Natural Gas Treatment: A Technology Update. Adsorption Processes for Natural Gas Treatment: a Technology Update, *Engelhard Brochure* **2004**.

(5) Sun, Q.; Wang, M.; Li, Z.; Li, P.; Wang, W. H.; Tan, X. J.; Du, A. J. Nitrogen Removal from Natural Gas using Solid Boron: A First-principles Computational Study. *Fuel* **2013**, *109*, 575-581.

(6) Tagliabue, M.; Farrusseng, D.; Valencia, S.; Aguado, S.; Ravon, U.; Rizzo, C.; Corma, A.; Mirodatos, C. Natural gas treating by selective adsorption: Material science and chemical engineering interplay. *Chem. Eng. J.* **2009**, *155*, 553-566.

(7) Batista, R. J. C.; Mazzoni, M. S. C.; Chacham, H. A theoretical study of the stability trends of boron nitride fullerenes. *Chem. Phys. Lett.* **2006**, *421*, 246-250.

(8) Alexandre, S. S.; Chacham, H.; Nunes, R. W. Structure and Energetics of Boron Nitride Fullerenes: The Role of Stoichiometry. *Phys. Rev. B* **2001**, *63*, 045402.

(9) Wen, S. H.; Deng, W. Q.; Han, K. L. Endohedral BN Metallofullerene $M@B_{36}N_{36}$ Complex as Promising Hydrogen Storage Materials. *J. Phys. Chem. C* **2008**, *112*, 12195-12200.

(10) Nigam, S.; Majumder, C. Magnetic Needles Encapsulated Inside $(BN)_{36}$ Cage: Prediction of Atomic, Electronic, and Magnetic Structure from First Principle Calculations. *Appl. Phys. Lett.* **2007**, *91*, 223112.

(11) Golberg, D.; Bando, Y.; Stephan, O.; Kurashima, K. Octahedral Boron Nitride Fullerenes Formed by Electron Beam Irradiation. *Appl. Phys. Lett.* **1998**, *73*, 2441-2443.

(12) Alexandre, S. S.; Mazzoni, M. S. C.; Chacham, H. Stability, Geometry, and Electronic Structure of the Boron Nitride $B_{36}N_{36}$ Fullerene. *Appl. Phys. Lett.* **1999**, *75*, 61-63.

(13) Zope, R. R.; Baruah, T.; Pederson, M. R.; Dunlap, B. I. Theoretical Infrared, Raman, and Optical Spectra of the $B_{36}N_{36}$ Cage. *Phys. Rev. A* **2005**, *71*, 025201.

(14) Wu, H. S.; Xu, X. H.; Strout, D. L.; Jiao, H. J. The Structure and Stability of $B_{36}N_{36}$ Cages: a Computational Study. *J. Mol. Model.* **2005**, *12*, 1-8.

(15) Narita, I.; Oku, T. Molecular Dynamics Calculation of H_2 Gas Storage in C_{60} and $B_{36}N_{36}$ Clusters. *Diam. Relat. Mater.* **2002**, *11*, 945-948.

(16) Ganji, M. D.; Yazdani, H.; Mirnejad, A. $B_{36}N_{36}$ Fullerene-like Nanocages: A Novel Material for Drug Delivery. *Physica E* **2010**, *42*, 2184-2189.

(17) Ganji, M. D.; Ghorbanzadeh, M.; Negaresh, M.; Najafi, A. A.; Rezvani, M.; Shokry, M. First-Principles Investigations on the Feasibility of the Boron Nitride Fullerene-Like $B_{36}N_{36}$ for Natural Gas Storage. *J. Comput. Theor. Nanosci.* **2011**, *8*, 862-866.

(18) Kanai, Y.; Khalap, V. R.; Collins, P. G.; Grossman, J. C. Atomistic Oxidation Mechanism of a Carbon Nanotube in Nitric Acid. *Phys. Rev. Lett.* **2010**, *104*, 066401.

(19) Ramesh, P.; Itkis, M. E.; Bekyarova, E.; Wang, F.; Niyogi, S.; Chi, X.; Berger, C.; de Heer, W.; Haddon, R. C. Electro-oxidized Epitaxial Graphene Channel Field-Effect Transistors with Single-Walled Carbon Nanotube Thin Film Gate Electrode. *J. Am. Chem. Soc.* **2010**, *132*, 14429-14436.

(20) Novoselov, K. S.; Geim, A. K.; Morozov, S. V.; Jiang, D.; Katsnelson, M. I.; Grigorieva, I. V.; Dubonos, S. V.; Firsov, A. A. Two-dimensional Gas of Massless Dirac Fermions in Graphene. *Nature* **2005**, *438*, 197-200.

(21) Delley, B. An Al-electron Numerical Method for Solving the Local Density Functional for Polyatomic Molecules. *J. Chem. Phys.* **1990**, *92*, 508-517.
(22) Delley, B. From Molecules to Solids with the DMol3 Approach. *J. Chem. Phys.* **2000**, *113*, 7756-7764.
(23) Perdew, J. P.; Burke, K.; Ernzerhof, M. Generalized Gradient Approximation Made Simple. *Phys. Rev. Lett.* **1996**, *77*, 3865-3868.
(24) Grimme, S. Semiempirical GGA-type Density Functional Constructed with a Long-range Dispersion Correction. *J. Comput. Chem.* **2006**, *27*, 1787-1799.
(25) Sun, Q.; Wang, M.; Li, Z.; Ma, Y. Y.; Du, A. J. CO_2 Capture and Gas Separation on Boron Carbon Nanotubes. *Chem. Phys. Lett.* **2013**, *135*, 59-66.
(26) Sun, Q.; Li, Z.; Searles, D. J.; Chen, Y.; Lu, G. Q.; Du, A. J. Charge Controlled Switchable CO_2 Capture on Boron Nitride Nanomaterials *J. Am. Chem. Soc.* **2013**, *135*, 8246-8253.
(27) Sun, Q.; Wang, M.; Li, Z.; Du, A.; Searles, D. J. Carbon Dioxide Capture and Gas Separation on B_{80} Fullerene. *J. Phys. Chem. C* **2014**, *118*, 2170-2177.
(28) Sun, Q.; Wang, M.; Li, Z.; Du, A.; Searles, D. J. A Computational Study of Carbon Dioxide Adsorption on Solid Boron. *Phys. Chem. Chem. Phys.* **2014**, *16*, 12695-12702.
(29) Mulliken, R. S. Electronic Population Analysis on LCAO-MO Molecular Wave Functions .1. *J. Chem. Phys.* **1955**, *23*, 1833-1840.
(30) Sun, Q.; Li, Z.; Wang, M.; Du, A.; Smith, S. C. Methane Activation on Fe_4 Cluster: A Density Functional Theory Study. *Chem. Phys. Lett.* **2012**, *550*, 41-46.
(31) Sun, Q.; Li, Z.; Du, A.; Chen, J.; Zhu, Z.; Smith, S. C. Theoretical Study of Two States Reactivity of Methane Activation on Iron Atom and Iron Dimer. *Fuel* **2012**, *96*, 291-297.
(32) Bader, R. F. W. *Atoms in Molecules: A Quantum Theory*; Oxford University Press: New York, 1990.
(33) Chu, S.; Majumdar, A. Opportunities and Challenges for a Sustainable Energy Future. *Nature* **2012**, *488*, 294-303.

TOC